Anal. Chem. **2008,** *80,* 7063–7067

Monitoring of Real-Time Streptavidin−Biotin Binding Kinetics Using Droplet Microfluidics

Monpichar Srisa-Art,[†] Emily C. Dyson,[†] Andrew J. deMello,*[,†] and Joshua B. Edel*[,†,‡]

Department of Chemistry, and Institute of Biomedical Engineering, Imperial College London, South Kensington, London, SW7 2AZ, United Kingdom

Rapid kinetic measurements are important in understanding chemical interactions especially for biological molecules. Herein, we present a droplet-based microfluidic platform to study streptavidin−biotin binding kinetics with millisecond time resolution. With integration of a confocal fluorescence detection system, individual droplets can be monitored and characterized online to extract kinetic information. Using this approach, binding kinetics between streptavidin and biotin were observed via fluorescence resonance energy transfer. The binding rate constant of streptavidin and biotin was found to be in a range of 3.0×10^6–4.5×10^7 M^{-1} s^{-1}.

Recently, droplet-based microfluidics have been developed to overcome the mixing and reagent dispersion problems associated with laminar flow-based microfluidics. By injecting laminar streams of aqueous reagents into an immiscible carrier fluid, droplets can be reproducibly generated with each droplet acting as a microreactor.[1] The aqueous solutions are localized within droplets and separated by the carrier fluid, leading to rapid mixing and no reagent dispersion. By inducing a winding part into microchannels, mixing inside droplets is enhanced by chaotic advection, which can be as fast as few milliseconds.[2] With these particular features, droplet microfluidics have been exploited to demonstrate a variety of chemical and biological processes[1] such as chemical synthesis,[3−6] protein crytallizations,[7−9] nanoparticle synthesis,[10,11] biological assays,[12] and cell studies.[13,14] Furthermore, droplet microfluidics have also been demonstrated for performing rapid kinetic measurements,[15] which are important in understanding chemical/biological reactivities especially for protein folding [16,17] and enzyme activities.[18−20] Due to high droplet generation frequencies, which can be up to kilohertz, online droplet detection is one of the most challenging in terms of extracting the huge amounts of information produced from this system. Recently, confocal spectroscopy was introduced as a highly efficient detection method within microfluidic droplets due to its sensitivity and speed.[21] To this end, we present a droplet microfluidics integrated with a confocal fluorescence detection system to perform rapid kinetic measurements. Reaction kinetics from each droplet can be accurately and precisely monitored and extracted in real time. Previously, we have demonstrated an application of this system by performing a high-throughput DNA binding assay. [21] In this article, binding kinetics of streptavidin and biotin system was studied using fluorescence resonance energy transfer (FRET).

Typical approaches used to perform kinetic measurements are stopped flow[22] and hydrodynamic focusing.[23] Unfortunately, stopped flow measurements require large sample volumes making this unsuitable for studying kinetics of biological samples produced in small quantities. With this is mind, microfluidic approaches using hydrodynamic focusing are widely used to study kinetics due to rapid mixing and low sample consumption. However, in order to obtain rapid mixing using this approach, high sheath flow rates are typically used. Consequently, one of the solutions needs to be used in excess to obtain rapid mixing. Therefore, hydrodynamic focusing is not suitable for kinetic measurements requiring concentrations variation of both reagents.

* To whom correspondence should be addressed. E-mail: a.demello@imperial.ac.uk; joshua.edel@imperial.ac.uk.
† Department of Chemistry.
‡ Institute of Biomedical Engineering.

(1) Huebner, A.; Sharma, S.; Srisa-Art, M.; Hollfelder, F.; Edel, J. B.; de Mello, A. J. *Lab Chip* **2008**, *8*, 1244–1254.
(2) Srisa-Art, M.; de Mello, A. J.; Edel, J. B. *Phys. Rev. Lett.* **2008**, *101*, 014502.
(3) Zourob, M.; Mohr, S.; Mayes, A. G.; Macaskill, A.; Pérez-Moral, N.; Fielden, P. R.; Goddard, N. J. *Lab Chip* **2006**, *6*, 296–301.
(4) Cygan, Z. T.; Cabral, J. T.; Beers, K. L.; Amis, E. J. *Langmuir* **2005**, *21*, 3629–3634.
(5) Carroll, N. J.; Rathod, S. B.; Derbins, E.; Mendez, S.; Weitz, D. A.; Pestev, D. N. *Langmuir* **2008**, *24*, 658–661.
(6) Liu, K.; Ding, H. J.; Chen, Y.; Zhao, X. Z. *Microfluidics Nanofluidics* **2007**, *3*, 239–243.
(7) Zheng, B.; Roach, L. S.; Ismagilov, R. F. *J. Am. Chem. Soc.* **2003**, *125*, 11170–11171.
(8) Zheng, B.; Gerdts, C. J.; Ismagilov, R. F. *Curr. Opin. Struct. Biol.* **2005**, *15*, 548–555.
(9) Yadav, M. K.; Gerdts, C. J.; Sanishvili, R.; Smith, W. W.; Roach, L. S.; Ismagilov, R. F.; Kuhn, P.; Stevens, R. C. *J. Appl. Crystallogr.* **2005**, *38*, 900–905.
(10) Nie, Z.; Xu, S.; Seo, M.; Lewis, P. C.; Kumacheva, E. *J. Am. Chem. Soc.* **2005**, *127*, 8058–8063.
(11) Hung, L. H.; Choi, K. M.; Tseng, W. Y.; Tan, Y. C.; Shea, K. J.; Lee, A. P. *Lab Chip* **2006**, *6*, 174–178.
(12) Zheng, B.; Ismagilov, R. F. *Angew. Chem., Int. Ed.* **2005**, *44*, 2520–2523.
(13) Huebner, A.; Srisa-Art, M.; Holt, D.; Abell, C.; Hollfelder, F.; Demello, A. J.; Edel, J. B. *Chem. Commun.* **2007**, 1218–1220.
(14) Huebner, A.; Olguin, L. F.; Bratton, D.; Whyte, G.; Huck, W. T.; DeMello, A. J.; Edel, J. B. *Anal. Chem.* **2008**, *10*, 3890–3896.
(15) Song, H.; Ismagilov, R. F. *J. Am. Chem. Soc.* **2003**, *125*, 14613–14619.
(16) Jackson, S. E. D.; Craggs, T.; Huang, J. R. *Expert Rev. Proteomics* **2006**, *3*, 545–559.
(17) Finkelstein, A. V.; Galzitskaya, O. V. *Phys. Life Rev.* **2004**, *1*, 23–56.
(18) Palmier, M. O.; Van Doren, S. R. *Anal. Biochem.* **2007**, *371*, 43–51.
(19) Walcott, S.; Lehman, S. L. *Biochemistry* **2007**, *46*, 11957–11968.
(20) Wiita, A. P.; Perez-Jimenez, R.; Walther, K. A.; Grater, F.; Berne, B. J.; Holmgren, A.; Sanchez-Ruiz, J. M.;; Fernandez, J. M. *Nature* **2007**, *450*, 124+
(21) Srisa-Art, M.; deMello, A. J.; Edel, J. B. *Anal. Chem.* **2007**, *79*, 6682–6689.
(22) Gomezhens, A.; Perezbendito, D. *Anal. Chim. Acta* **1991**, *242*, 147–177.
(23) Knight, J. B.; Vishwanath, A.; Brody, J. P.; Austin, R. H. *Phys. Rev. Lett.* **1998**, *80*, 3863–3866.

10.1021/ac801199k CCC: $40.75
Published on Web 08/20/2008

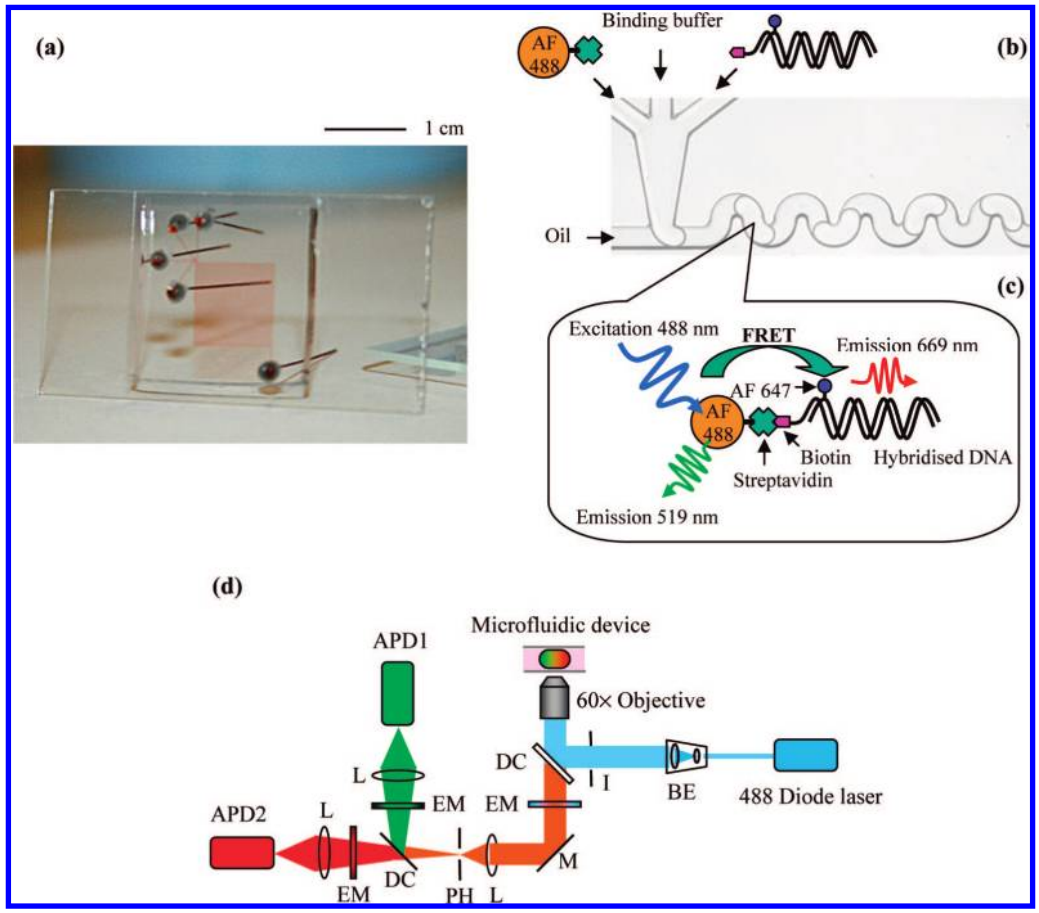

Figure 1. (a) Image of the microfluidic device. The 50-μm-square cross-section microchannel network consists of 4 inlets and 1 outlet. (b) A schematic of the microfluidic device setup for FRET kinetic experiments. The AF 488 conjugated streptavidin solution is flowing into a left inlet, while AF 647 and biotin-labeled DNA solution is pumping through the right inlet. The binding buffer is delivered into the middle inlet. (c) Schematic of the FRET process. The acceptor is linked to the donor via the streptavidin−biotin linkage, resulting in FRET. (d) A schematic of the optical fluorescence detection system used (APD = avalanche photodiode detector; BE = beam expander; DC = dichroic mirror; EM = emission filter; I = iris; L = lens; M = mirror; and PH = pinhole).

Although mixing inside droplets is not as fast as hydrodynamic focusing, kinetic measurements using droplet microfluidics have shown some advantages in terms of reaction time scales, low sample consumption due to small droplet volumes (10^{-9}–10^{-12} L), and no reagent dispersion, which allows reaction times to be calculated at any distance. Thus, reactions can be precisely and accurately controlled and monitored at desired time scales. For this reason, droplet microfluidics is an alternative and promising technique to study kinetics. An elegant example was initially demonstrated by Song et al.[15] Using submicroliter volumes of solution, rapid single-turnover kinetics of ribonuclease A (RNase A) was measured with better than millisecond resolution. The kinetic measurements were performed by monitoring fluorescence intensity arising from the cleavage of a fluorogenic substrate by RNase A. Fluorescence images were taken using a CCD camera at different time points. The images were then analyzed using image software to build intensity profiles to extract kinetic data. Although kinetic information can be extracted by analyzing fluorescence images from a CCD camera, this method mainly relies on selected areas of interest and uniform illumination of the light source. In addition, a high-speed CCD camera is not fast enough to sensitively interrogate each droplet to obtain kinetic data. Hence, a highly efficient detection system, which can monitor reaction kinetics in real time, is key.

Typically, determination of the biding rate constant for biological molecules is more difficult than that of the dissociation rate constant as most biological molecules exhibit binding interactions much faster than dissociation processes, especially streptavidin−biotin binding demonstrating a high binding constant of $\sim 10^{15}$ M^{-1}.[24−27] Accordingly, it is more practical to carry out experiments to measure the dissociation rate constant. However, due to rapid mixing, the droplet system can be suitably implemented to determine binding kinetics as is demonstrated in this article.

EXPERIMENTAL SECTION

Device Fabrication. Figure 1a shows an image of a PDMS microfluidic device, having 50.0-μm-wide, 50.0-μm-deep, and ~44.0-cm-long channels. Fabrication of these devices was performed as described previously.[21] A winding part of the primary microchannel was integrated in order to induce rapid mixing due to chaotic advection within each droplet, which allows for kinetic measurements in millisecond time scales.

Detection System. The completed microfluidic device was placed onto a controllable stage (ProScan II, Prior Scientific) of

(24) Piran, U.; Riordan, W. J. *J. Immunol.l Methods* **1990**, *133*, 141–143.
(25) Bayer, E. A.; Wilchek, M. *Methods Enzymol.* **1990**, *184*, 49–51.
(26) Chilkoti, A.; Stayton, P. S. *J. Am. Chem. Soc.* **1995**, *117*, 10622–10628.
(27) Livnah, O.; Bayer, E. A.; Wilchek, M.; Sussman, J. L. *Proc. Natl. Acad. Sci. U. S. A.* **1993**, *90*, 5076–5080.

an Olympus IX71 microscope appropriately aligned with a custom-built confocal spectrometer (Figure 1d). The confocal setup consists of a 488-nm diode laser (Coherent UK Ltd.). The laser beam was aligned into the microscope body using beam steering optics. A filter wheel was installed to attenuate the laser beam, after which the light was expanded by a beam expander (Thorlabs) to entirely fill the back aperture of a 60× water immersion microscope objective (Olympus). A dichroic mirror (z488rdc, Chroma Technology Corp.) is used to reflect the 488-nm laser beam into the objective lens. This brings the laser light to a tight focus within the microfluidic channels. Fluorescence emission is collected with the same objective and transmitted through the same dichroic mirror. An emission filter (z488lp; Chroma Technology Corp.) removes any residual excitation light, and a plano-convex lens (+50.2F; Newport Ltd.) focuses the fluorescence onto a 75-μm precision pinhole (Melles Griot) positioned in the focal plane of the microscope objective. Another dichroic mirror (630dcxr, Chroma Technology Corp.) is then used to split the fluorescent signal onto two avalanche photodiodes (AQR-141, EG&G, Perkin-Elmer). Fluorescence reflected by the dichroic mirror is further filtered by an emission filter (hq540/80m, Chroma Technology Corp.) and focused by a plano-convex lens (f = 30.0, i.d. 25.4 mm, Thorlabs) onto the first avalanche photodiode (green detector). Fluorescence passing through the dichroic mirror is filtered by an emission filter (hq640lp, Chroma Technology Corp.) and then focused by another plano-covex lens onto the second avalanche photodiode (red detector). Dual color detection was implemented for FRET-based experiments where the donor and acceptor fluorophores are recorded in distinct detection channels. Both detectors are coupled to a multifunction DAQ device for data logging (PCI 6602, National Instruments) and have submicrosecond time resolution per channel.

Sample Preparation and Operation. The FRET system used for kinetic measurements was the same as in the previous work.[21] Briefly, the donor was Alexa Fluor 488 conjugated streptavidin (St-AF 488) and the acceptor was Alexa Fluor 647 (AF 647) internally labeled on one DNA strand, which the complementary strand was modified with biotin. Consequently, hybridized DNA consisted of AF 647 on one strand and biotin on the complementary strand.

Precision syringe pumps (PHD 2000, Harvard Apparatus) were used to deliver reagent solutions. All aqueous solutions were pumped into the microfluidic channels using 250-μL gastight syringes (SGE Europe Ltd.), whereas a 2.5-mL gastight syringe was used to deliver the continuous oil phase consisting of a 10:1 (v/v) mixture of perfluorodecalin and 1*H*,1*H*,2*H*,2*H*-perfluorooctanol. All liquids were filtered using 0.2-μm syringe filters (Pall Corp.) before use.

RESULTS AND DISCUSSION

Streptavidin−Biotin Binding. Microdroplets were formed using flow rates of 1.5 μL min^{-1} for both the aqueous (total of 3 inlets) and oil phases. The St-AF 488 and AF 647 and biotin-labeled hybridized DNA solutions were pumped separately through the aqueous inlets. A pH 8.0 binding buffer, consisting of 100 mM Tris-HCl, 10 mM NaCl, and 3 mM $MgCl_2$, was delivered into the middle aqueous inlet in order to prevent the reagents from coming into contact prior to droplet formation and to allow for on-chip dilution. Thus, mixing and binding of streptavidin and DNA only occurs inside the formed droplet. A schematic setup of this experiment is depicted in Figure 1b. Upon binding of biotin to streptavidin, FRET is observed due to the close proximity of both the acceptor and donor fluorophores.

Table 1. Experimental Conditions for the FRET Kinetic Mesurements

flow rate (μL min^{-1})			concentration (nM)		CR
streptavidin	DNA	buffer	streptavidin	DNA	
0.3	0.3	0.9	22.0	20.0	0.91
0.3	0.4	0.8	22.0	26.7	1.21
0.3	0.5	0.7	22.0	33.3	1.52
0.3	0.6	0.6	22.0	40.0	1.82
0.3	0.7	0.5	22.0	46.7	2.12
0.3	0.8	0.4	22.0	53.3	2.42
0.3	0.9	0.3	22.0	60.0	2.73

The binding kinetic measurements were performed by fixing the donor-labeled streptavidin concentration and varying the acceptor-labeled DNA concentration. This was achieved by keeping the flow rate of 110 nM donor-labeled streptavidin constant at 0.3 μL min^{-1}, resulting in a concentration of 22.0 nM, while varying the flow rates of 100 nM biotin and acceptor-labeled DNA. The DNA flow rates were changed from 0.3 to 0.9 μL min^{-1} (using a step of 0.1 μL min^{-1}), giving a concentration range from 20.0 to 60.0 nM. Consequently, concentration ratios (CRs), defined as the ratio of DNA concentration to streptavidin concentration, were changed from 0.91 to 2.73. Accordingly, the flow rate of the binding buffer at the middle inlet was adjusted to maintain a total aqueous flow rate of 1.50 μL min^{-1}. The experimental conditions are expressed in Table 1.

Since AF 488 emits green fluorescence with a peak maximum at 519 nm, upon binding of streptavidin to biotin, some energy is transferred to AF 647. Red fluorescence, detected by the red detector, at wavelengths between 650 and 710 nm was obtained from AF 647 emission only as a result of FRET. This FRET process was shown in Figure 1c. Thus, two fluorescence signals (from AF 488 and AF 647) from each droplet were detected simultaneously using separate APD detectors and recorded for 60 s using 50-μs bin times. The fluorescence intensity of both the acceptor and donor, monitored at different points down the length of the channel, was used to extract binding kinetics.

Panels a and b in Figure 2 show burst height and area distributions of red fluorescence (FRET) signals for the first few detection points. Both are perfectly modeled by Gaussian distributions and clearly show an increase in signal as the droplet moves further down the channel. This is due to the progressive binding between streptavidin and biotin, causing more linkages between the FRET donor and acceptor. Hence, the energy transferred between the two was greater and the signal increased.

The binding kinetics could be extracted by plotting FRET efficiency as a function of time, which is presented in Figure 3a. The FRET efficiencies from different time points were calculated using

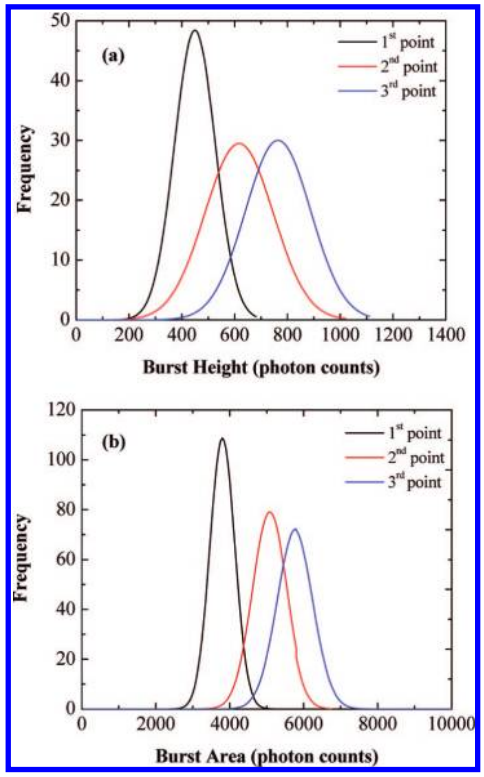

Figure 2. Burst height (a) and burst area (b) distributions of red fluorescence (FRET) signals from the first few data points. The first point was monitored at 0.41 s after droplet formation. The second and third points are 0.93 and 1.19 s, respectively.

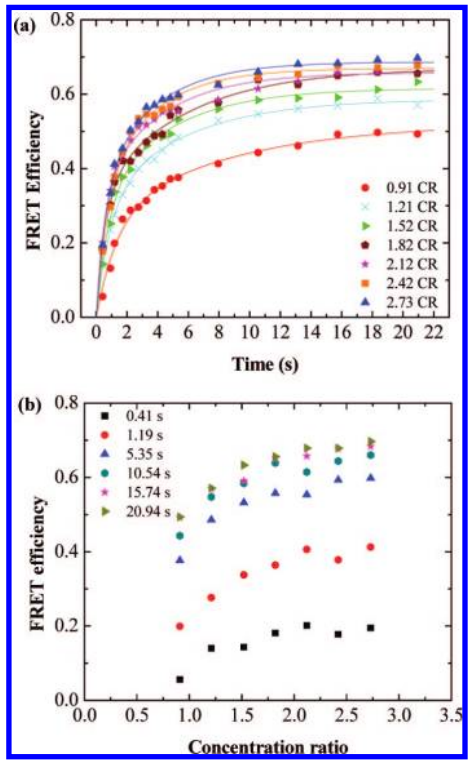

Figure 3. (a) Binding kinetic plots illustrating the FRET efficiency as a function of time when fixing streptavidin concentration at 22.0 nM. The binding kinetics monitored at different time points was investigated using the concentration ratios ranging from 0.91 to 2.73. Data was fitted using a biexponential model. (b) Plots of FRET efficiency against the concentration ratio at different time points.

$$E_{\mathrm{FRET}} = \frac{I_{\mathrm{A}}}{I_{\mathrm{A}} + I_{\mathrm{D}}} \tag{1}$$

where I_{D} and I_{A} are the fluorescence intensities of the donor and acceptor, respectively.[21]

As the detection probe volume, set at a channel depth of 25 μm, was positioned at points down the length of the channel, the FRET efficiency increased rapidly at the beginning of the curves (for the first 5 s) and remained stable after ~10 s. Comparison of data measured at different concentration ratios demonstrates that using a higher binding ratio resulted in a shift toward higher FRET efficiencies due to the increased number of the acceptors linked to the donors. In addition, at the low concentration ratios (0.91−1.52), increasing the concentration ratio showed significant changes in FRET efficiency. However, only a slight increase in the efficiency was observed at concentration ratios from 1.82 to 2.73, due to the limitation of biotin binding sites on the streptavidin. The highest FRET efficiency of ~0.70 was obtained from the concentration ratio of 2.73.

In addition, the binding kinetics was also determined from a plot of FRET efficiency against the concentration ratio at different time points. This plot, shown in Figure 3b, demonstrates kinetic behavior for each binding ratio when the reaction moved downstream. As seen from the graphs at a single concentration ratio, the FRET efficiency rose sharply for the first 5 s, indicating fast kinetics. Afterward, the FRET efficiency increased slowly and remained stable. A similar trend of the FRET efficiency at every concentration ratio was obtained when the reaction was monitored after 10 s. These confirm fast binding kinetics between streptavidin and biotin and also imply that the complete binding of our analytes occurs in a 10 s time frame. All curves reach a plateau at a concentration ratio of ~2.0, which corresponds well to the binding ratio previously obtained by our group.[21]

Binding Rate Constant. Normally, a simple interaction of two biomolecules can be described using the following model:[28]

$$\mathrm{S} + \mathrm{L} \underset{k_{-1}}{\overset{k_1}{\rightleftharpoons}} SL \tag{2}$$

Here S and L symbolize two biomolecules. k_1 and k_{-1} are the binding and dissociation rate constants, respectively. The binding rate can be determined from the formation of SL over time. Ideally, this binding interaction should be described by a monoexponential growth equation or the integrated rate equation of the pseudo-first-order reaction:[28]

$$\mathrm{SL}_t = \mathrm{SL}_{\max}(1 - \mathrm{e}^{-k_{\mathrm{obs}}t}) \tag{3}$$

In this equation, SL_t is the amount of product at a time point, $\mathrm{SL}_{\max}$ is the maximum amount (the plateau value) and k_{obs} is an observed rate constant for each condition. The k_{obs}, a concentration-dependent value; is related to k_1 from the following expression:

$$k_{\mathrm{obs}} = k_1[\mathrm{L}] + k_{-1} \tag{4}$$

To extract k_1, the values of k_{obs} are plotted against varied concentrations of L. According to eq 4, this plot gives a linear relationship, with the slope equals to k_1 and the y-intercept represents k_{-1} (the dissociation rate constant).

However, in many cases including our case, kinetic behaviors of two-biomolecule binding cannot be well explained using the monoexponential expression (eq 3), but rather can more accurately be described by a biexponential model:[29,30]

$$SL_t = A_1[1 - e^{(-k_{obs1}t)}] + A_2[1 - e^{(-k_{obs2}t)}] \quad (5)$$

where k_{obs1} and k_{obs2} are observed binding rate constants of each process. A_1 and A_2 represent the amplitudes of the each process.

This model, expressing a biphasic interaction, indicates an unusual bimolecular interaction in which at least two processes are involved. The biphasic dissociation or association can occur due to heterogeneity of analytes or multiple binding sites causing different affinities.[31]

For streptavidin and biotin interaction, the reaction was categorized as biphasic due to multiple biotin binding sites on a streptavidin molecule.[32,33] Hence, to extract the binding rate constant of our streptavidin and biotin system, all kinetic data in Figure 3a was fit by nonlinear regression using eq 5, in which SL is the FRET efficiency for our experiments. As seen from Figure 3a, this model provides perfect fitting for every concentration ratio. Observed rate constants (k_{obs1} and k_{obs2}) for each condition were obtained from the fitting. To extract the binding rate constants (k_1 and k_2), the k_{obs1} and k_{obs2} values were plot separately against the concentration of DNA, as shown in Figure 4, using eq 4. Both graphs show linear trends with R^2 values of 0.9847 and 0.9456 for k_{obs1} and k_{obs2} plots, respectively. The slopes obtained from these plots are equal to 4.5×10^7 and 3.0×10^6 M^{-1} s^{-1}, which are k_1 and k_2, respectively. It can be seen that k_2, representing binding kinetics of the second process, was found to be lower than k_1 of the first process. This could be due to steric hindrance from the first biotin binding because our biotin molecule was attached to double stranded DNA.

Buranda et al. found the binding rate constant of $\sim 10^7$ for biotin binding to the first binding site of a streptavidin molecule.[33] They noticed that the binding rate for the second biotin molecule was decreased due to steric hindrance. In addition, the association rate constant of 7×10^7 M^{-1} s^{-1} was reported for biotin and avidin,

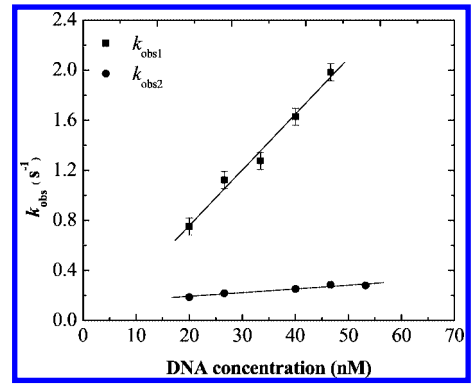

Figure 4. Observed rate constants (k_{obs}) against the DNA concentration. The k_{obs} values were obtained from a nonlinear least-squares fit.

in which the binding is stronger than that of biotin and streptavidin.[25] Due to a relatively slow process, therefore, there were some papers investigating the dissociation rate constant between streptavidin and biotin. The dissociation rate constant of 2.4×10^{-6} s^{-1} was reported for underivertized streptavidin, which was 30-fold higher than that observed from avidin (7.5×10^{-8} s^{-1}).[24] From previous results, the binding rate constants are slightly different, depending on streptavidin and biotin systems and conditions applied to the binding. Therefore, it is possible that the rate constant for streptavidin and biotin binding could be varied by 1 order of magnitude.[25] Hence, the binding rate constants of 3.0×10^6 and 4.5×10^7 M^{-1} s^{-1} obtained from our streptavidin and biotin system are in agreement with previous studies.

CONCLUSIONS

Droplet microfluidics integrated with a confocal fluorescence detection system has been successfully used to perform online kinetic measurements with millisecond time scales. The binding rate constant of streptavidin and biotin of our particular system was found to be in a range of 3.0×10^6–4.5×10^7 M^{-1} s^{-1}. Using the approach described, kinetic studies of more complex systems such as high-throughput protein folding/unfolding will be possible.

ACKNOWLEDGMENT

This work was supported by the EPSRC and the RCUK Basic Technology Programme. M.S.-A. acknowledges the Royal Thai Government for provision of a research scholarship.

Received for review June 12, 2008. Accepted June 30, 2008.

AC801199K

(28) Goodrich, J. A.; Kugel, J. F. *Binding and Kinetics for Molecular Biologists*; Cold Spring Harbor: New York, 2007.
(29) Oshannessy, D. J.; Brighamburke, M.; Soneson, K. K.; Hensley, P.; Brooks, I. *Anal. Biochem.* **1993**, *212*, 457–468.
(30) Edwards, P. R.; Leatherbarrow, R. J. *Anal. Biochem.* **1997**, *246*, 1–6.
(31) Edwards, P. R.; Gill, A.; Pollardknight, D. V.; Hoare, M.; Buckle, P. E.; Lowe, P. A.; Leatherbarrow, R. J. *Anal. Biochem.* **1995**, *231*, 210–217.
(32) Gonzalez, M.; Bagatolli, L. A.; Echabe, I.; Arrondo, J. L. R.; Argarana, C. E.; Cantor, C. R.; Fidelio, G. D. *J. Biol. Chem.* **1997**, *272*, 11288–11294.
(33) Buranda, T.; Jones, G. M.; Nolan, J. P.; Keij, J.; Lopez, G. P.; Sklar, L. A. *J. Phys. Chem. B* **1999**, *103*, 3399–3410.